

MOUNT FUJI [CI] LINE SURVEY

TAKESHI SAKAI^{1,3}, SATOSHI YAMAMOTO^{2,3}

¹Nobeyama Radio Observatory, Minamimaki, Minamisaku Nagano, 384-1305, Japan,
E-mail: sakai@nro.nao.ac.jp

²Department of Physics, The University of Tokyo, 7-3-1, Hongo, Bunkyo-ku, Tokyo 113-0033, Japan
E-mail: yamamoto@phys.s.u-tokyo.ac.jp

³Mount Fuji Submillimeter-wave Telescope Group
(Received February 1, 2005; Accepted March 15, 2005)

ABSTRACT

We have constructed the Mount Fuji submillimeter-wave telescope at Nishiyasugawara (alt. 3725 m) near the summit of Mt. Fuji (alt. 3774 m). Thanks to the excellent condition of Mt. Fuji, we have successfully carried out the [CI] survey toward more than 40 square degrees of sky, including Orion MC, Taurus MC, Rosetta MC, DR 15, DR 21, NGC 1333, NGC 2264, W 3, W 44, W 51, L 134, ρ -Oph. Our [CI] survey have revealed that the [CI] 492 GHz emission widely extends to the molecular clouds. The spatial and velocity structures of the [CI] 492 GHz emission resemble those of $^{13}\text{CO } J=1-0$ in many molecular clouds, implying that [CI] 492 GHz and $^{13}\text{CO } J=1-0$ are emitted from the same gas. The column density of C^0 linearly correlates with that of CO up to high A_V , suggesting that C^0 exist in the deep interior of molecular clouds. In several regions, we have found that the distributions of C^0 and CO are different from each other. The C^0 -rich area is found in the Hiele's cloud 2. The $\text{C}^+/\text{CO}/\text{C}^0$ configuration is found in DR 15, ρ -Oph, M 17, Orion KL, and NGC 1333. These results indicate that an origin of C^0 is unrelated with the photodissociation process. We discuss the observed C^0 distributions in relation to the non-equilibrium chemistry.

Key words : submillimeter-wave telescope — ISM: molecules — ISM: atoms — submillimeter [CI] lines

I. INTRODUCTION

In interstellar space, the gas phase carbon is mainly in three forms; carbon ion (C^+), carbon monoxide (CO) and neutral carbon atom (C^0). The main forms of carbon changes with the evolution of a interstellar cloud. Since the ionization potential of the carbon atom (11.6 eV) is lower than that of the hydrogen atom (13.6 eV), the carbon atom can be easily ionized by the interstellar UV radiation. Thus C^+ is abundant in a diffuse cloud. With increasing density of a cloud, the interstellar UV radiation is shielded by dust grains, and consequently, the main form of carbon changes from C^+ to C^0 and then to CO. In the UV-shielded region, binary reactions, such as neutral-neutral or ion-neutral reactions, are responsible chemical processes, and C^0 is slowly converted to CO toward its chemical equilibrium with a time scale of $\sim 10^6$ yr (e.g. Suzuki et al. 1992). This is comparable with the dynamical time scale of molecular cloud cores. Hence we expect the C^0 -rich state in the early stage of cloud formation, and the C^0/CO abundance ratio may be used as a "chemical clock". Therefore, the C^0 observations are useful to investigate the evolution of molecular clouds.

C^0 has two transitions in the submillimeter-wave band; $\text{C}^0 \ ^3P_1-^3P_0$ ([CI] 492 GHz) and $\text{C}^0 \ ^3P_2-^3P_1$ ([CI]

809 GHz). Since the critical density of [CI] 492 GHz is about 10^3 cm^{-3} and the energy of 3P_1 is 24 K, it can be easily excited in molecular clouds. Thus the [CI] 492 GHz line is useful to reveal the distribution of C^0 in molecular clouds. The [CI] 809 GHz line traces warm regions, because of relatively high energy of 3P_2 (62 K). From the both [CI] lines, we can derive the optical depth, excitation temperature, and column density under the LTE assumption.

The [CI] observations have been carried out by using the JCMT 15 m telescope and the CSO 10.4 m telescope. However, since their beam size are very small (15" and 9".8 at 492 GHz for CSO and JCMT, respectively), large scale mappings are not practical. In order to reveal the role of C^0 in the molecular cloud evolution, large scale mapping observations are crucial. For this purpose, a small sized telescope, whose beam size is relatively large, is useful. With this motivation in mind, we developed the Mount Fuji submillimeter-wave telescope for the exclusive use of the [CI] line observations.

II. THE MOUNT FUJI SUBMILLIMETER-WAVE TELESCOPE

In 1998, the Mount Fuji submillimeter-wave telescope was installed at Nishiyasugawara (alt. 3725 m) near the summit of Mt. Fuji (alt. 3774 m), which is the highest mountain in Japan. Before the installation, Sekimoto et al. (1996) observed the 220 GHz opacity at the summit of Mt. Fuji, and revealed that the 220

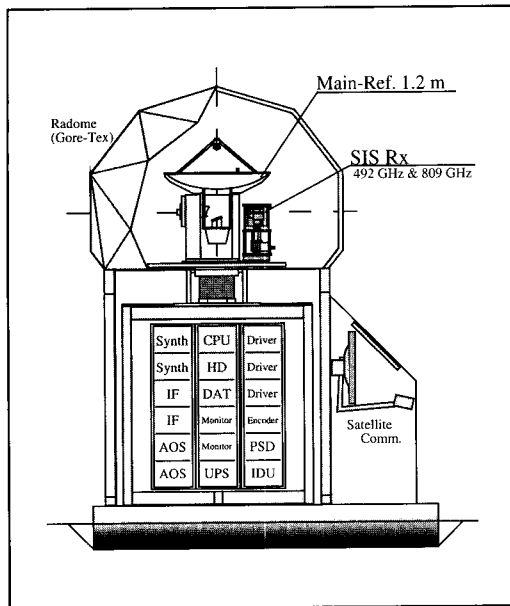


Fig. 1.— A schematic illustration of the inside of the Mount Fuji submillimeter-wave telescope.

GHz opacity is lower than ~ 0.06 for a significant fraction ($\sim 45\%$) of the time from November 1994 to March 1995. The 220 GHz opacity of 0.06 corresponds to the 492 GHz opacity of 1.0. This result indicates good observing condition at the submillimeter-wave region from Mt. Fuji.

Observation season for the [CI] lines with the Mount Fuji submillimeter-wave telescope is usually from November to March. During this period, it is difficult to climb the mountain because of heavy snow and ice. We operate the telescope through the internet from the University of Tokyo by using the satellite communication system.

Figure 1 shows a schematic illustration of the inside of the Mount Fuji submillimeter-wave telescope. The telescope is enclosed in a radome with the Gore Tex membrane, whose transmission efficiency is 81% for 492 GHz. The main dish and the receiver dewar are installed in the upper cabin. The main dish has a diameter of 1.2 m. The surface accuracy is $10\ \mu\text{m}$. The beam size is $2'.2$ at 492 GHz.

For receivers of the Mount Fuji submillimeter-wave telescope, we use the Nb-based SIS devices, the distributed junctions (DJ) type (Shi et al. 1998) and parallel-connected twin junction (PCTJ) type (Shi et al. 1997) devices fabricated in the Nobeyama Radio Observatory. The receiver noise temperature is 120 K and 680 K for the 492 GHz and 809 GHz bands, respectively.

The backend is an acousto-optical spectrometer (AOS), whose center frequency is 2.15 GHz and band width is 900 GHz for 1024 channel. The effective resolution is 1.6 MHz, which corresponds to the $1\ \text{km s}^{-1}$ resolution at 492 GHz. The obtained data are accumulated with

the simple adder, and the integrated data are sent to a host computer through the GPIB interface.

The position-switch and frequency-switch modes can be used. We employ a single load chopper wheel method for all observations. We obtain the value of η_{MB}^{eff} by observing the full moon. η_{MB}^{eff} is estimated to be 0.45 for 492 GHz. Pointing calibrations are carried out by observing the continuum emission from the full moon and the sun at 492 GHz every month. The pointing accuracy is kept to be better than $20''$ in r.m.s. We also check the pointing accuracy by observing the 3×3 positions in Orion KL and M17 every observing day. Other details of the telescope are described elsewhere (Sekimoto et al. 2000).

III. [CI] LINE SURVEY

We have successfully carried out the large scale [CI] mapping observations in five seasons. The surveyed area in the [CI] 492 GHz line is more than 40 square degree of sky, including 9 massive star forming regions (Orion MC; Ikeda et al. 1999, 2002, DR 15; Oka et al. 2001, DR 21, NGC 2264, M17; Sekimoto et al. 1999, W 3; Sakai et al. 2005, W 44, W 51; Arikawa et al. 1999, Rosetta MC), 2 intermediate-mass star forming regions (NGC 1333; Oka et al. 2004, ρ -Oph; Kamegai et al. 2003), and 2 dark clouds (Taurus MC; Maezawa et al. 1999, L134 complex). We have also mapped several regions in the [CI] 809 GHz line; Orion KL (Yamamoto et al. 2001; Kuboi et al. 2005), M 17, NGC 2024, and DR 21.

(a) [CI] Distributions

So far, it was thought that C^0 is abundant in the thin layer of the cloud surface illuminated by the interstellar UV radiation (e.g. Tielens & Hollenbach, 1985). Therefore the [CI] mapping observations have been biased on the small areas around UV sources. Our large scale [CI] mapping observations have revealed that the [CI] emission is distributed in the almost whole region of a molecular cloud.

Ikeda et al. (1999, 2001) mapped the Orion A and Orion B molecular clouds in the [CI] 492 GHz line. Figure 2 shows the [CI] contour map overlaid on the Digital Sky Survey optical image toward the Orion A molecular cloud. The [CI] emission is distributed not only near the HII region but also in the dark cloud. They found that the overall spatial and velocity structures of the [CI] emission are similar to those of the $^{13}\text{CO } J=1-0$ emission. Such a similarity between [CI] 492 GHz and $^{13}\text{CO } J=1-0$ has been found in many molecular clouds, such as W 3, DR 21, NGC 2264, Rosetta MC, and M 17. This similarity may suggest that the emitting region of the [CI] line is same as that of the $^{13}\text{CO } J=1-0$ line.

On the other hand, the distributions in a small scale are slightly different between C^0 and CO. Oka et al. (2001) observed the DR 15 region in the [CI] and CO

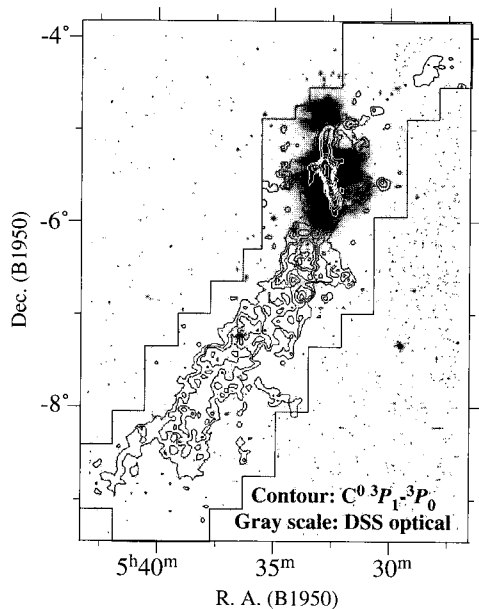


Fig. 2.— Integrated intensity [CI] contour map overlaid on the Digital Sky Survey optical image (gray scale) toward the Orion A molecular cloud (Ikeda et al. 1999, 2001).

lines, and found that the [CI] intensity peaks behind the dense core from the ionization front (Fig. 3). In the steady state models (e.g. Tielens & Hollenbach, 1985), the [CI] peak should exist between the ionization front and the dense core. A similar trend has been observed in ρ -Oph (Kamegai et al. 2003), M 17, NGC 1333 (Oka et al. 2004), and Orion KL (Kuboi et al. 2005). Kuboi et al. (2005) mapped the Orion-KL region in the [CI] 809 GHz line, and derive the C^0 column density from the [CI] 492 GHz and 809 GHz intensities with the LTE assumption. They confirm that the C^0 abundance peak is located behind the dense core from the ionization front. These results indicate that the "inverted" layering ($C^+ / CO / C^0$) does not originate from spatial geometrical arrangements specific to individual regions, but is rather ubiquitous in molecular clouds illuminated by the strong UV radiation.

Oka et al. (2004) show that the time-dependent chemical model can explain the "inverted" layering. Since the chemical time scale depends on density, C^0 is converted to CO more quickly in the dense cores than in the diffuse envelope. Therefore, C^0 peaks in the relatively diffuse region behind the dense cores.

(b) C^0 / CO Abundance Ratio

We found that the column density of C^0 linearly correlates with that of CO up to high A_V in many molecular clouds. The linear correlation between $N(C^0)$ and $N(CO)$ indicates that C^0 exist in the deep inside of molecular cloud. This cannot be explained with the steady state chemical models. Thus the origin of C^0 is unrelated to the photodissociation process, and it is

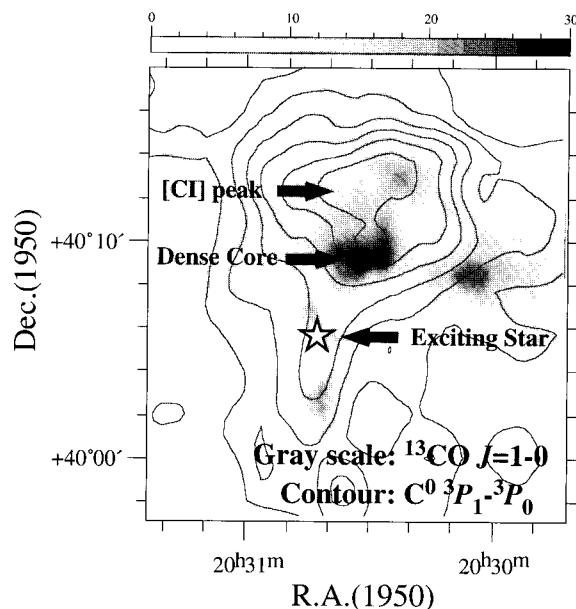


Fig. 3.— Integrated intensity [CI] contour map overlaid on the gray scale ^{13}CO map toward DR 15 (Oka et al. 2001).

likely that the molecular clouds do not reach the chemical equilibrium.

We have proposed that the C^0 -rich state may be observed in the early stage of cloud evolution. Maezawa et al. (1999) found the C^0 -rich area in the Heiles' cloud 2 (HCL 2) in Taurus molecular cloud (Fig. 4). The $[C^0]/[CO]$ ratio is as high as 0.8 in the C^0 -rich area, whereas it is ~ 0.1 in the dense cores. The $[C^0]/[CO]$ ratio in the C^0 -rich area is comparable with that in the translucent cloud (> 1), although the cloud has A_V of 8 mag. The C^0 -rich area is located between the dense cores and translucent cloud.

The chemical composition of TMC-1 in the HCL 2 is well studied, where the carbon chain molecules are spatially anti-correlated with SO, NH_3 , and N_2H^+ (e.g. Hirahara et al. 1992, 1995). For example, the peak of CCS is located to the 7' north of the peak of NH_3 (see Fig. 4). This is interpreted as the difference in the age of molecular cloud cores; the south part is more evolved than the north part (Hirahara et al. 1992). The C^0 -rich area is located to the south of the CCS peak. The arrangement of NH_3 , CCS, and C^0 , going from north to south, is consistent with the time-dependent chemistry. Therefore it is possible that the C^0 -rich area is in the early stage of chemical evolution and that HCL 2 has evolved from north to south.

We have revealed the [CI] 492 GHz distribution toward the W 3 GMC (Sakai et al. 2005). The [CI] emission peaks in three star forming clouds; W 3(Main), W 3(OH) and AFGL 333. The $[C^0]/[CO]$ ratio is found to be high in the AFGL 333 cloud as compared with the W 3(Main) and W 3(OH) clouds. The $[CCS]/[N_2H^+]$ ratio, which is often used as a chemical clock, is also

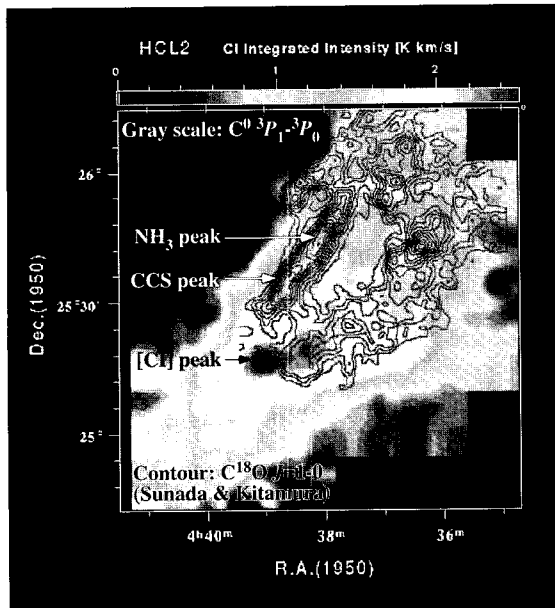


Fig. 4.— Integrated intensity [CI] map (gray) overlaid on the $C^{18}O$ contour map toward HCL 2 (Maezawa et al. 1999).

found to be high in the AFGL 333 cloud. These results indicate that the AFGL 333 cloud is chemically young.

A clumpy structure of molecular clouds has been discussed to explain the observed [CI] emission (e.g. Meixner & Tielens, 1993, 1995). However, the high $[C^0]/[CO]$ and $[CCS]/[N_2H^+]$ ratios in the AFGL 333 cloud may not be explained with the clumpy PDR models. Bergin et al. (1997) point out that a low filling factor of dense clump cannot produce the abundance of most molecules, because the UV radiation, which penetrates to the deep inside of a molecular cloud through the interclump medium, destroys various molecules. Thus, the time-dependent chemistry is necessary in order to explain the abundances of C^0 .

IV. SUMMARY

We have revealed the [CI] distribution in many molecular clouds by using the Mount Fuji submillimeter-wave telescope. The observed [CI] features, such as the $C^+/CO/C^0$ configuration and the linear correlation between $N(C^0)$ and $N(CO)$, can be explained with the time-dependent chemical model. Thus the non-equilibrium chemistry is important for the origin of a major part of C^0 in molecular clouds, and the C^0/CO ratio is useful to investigate the evolutionary stages of molecular clouds.

ACKNOWLEDGEMENTS

The authors are grateful to the members of the Mount Fuji submillimeter-wave telescope group. This study is supported by Grant-in-Aid from the Min-

istry of Education, Science, and Culture (07CE2002, 14204013, and 15071201).

REFERENCES

- Arikawa, Y., Tatematsu, K., Sekimoto, Y., et al., 1999, Star Formation 1999, Proceedings of Star Formation 1999, held in Nagoya, Japan, June 21 - 25, 1999, Editor: T. Nakamoto, Nobeyama Radio Observatory, 88-89
- Bergin, E. A., Goldsmith, P. F., Snell, R. L., & Langer, W. D., 1997, *ApJ*, 482, 285
- Hirahara, Y., Suzuki, H., Yamamoto, S., et al., 1992, *ApJ*, 394, 539
- Hirahara, Y., Masuda, A., Kawaguchi, K., et al., 1995, *PASJ*, 47, 845
- Ikeda, M., Maezawa, H., Ito, T., et al., 1999, *ApJL*, 527, L59
- Ikeda, M., Oka, T., Tatematsu, K., Sekimoto, Y., & Yamamoto, S., 2002, *ApJS*, 139, 467
- Kamegai, K., Ikeda, M., Maezawa, H., et al., 2003, *ApJ*, 589, 378
- Kuboi et al., 2005, *ApJ*, submitted.
- Maezawa, H., Ikeda, M., Ito, T., et al., 1999, *ApJL*, 524, L129
- Meixner, M., & Tielens, A. G. G. M., 1993, *ApJ*, 405, 216
- Meixner, M., & Tielens, A. G. G. M., 1995, *ApJ*, 446, 907
- Oka, T., Yamamoto, S., Iwata, M., et al., 2001, *ApJ*, 558, 176
- Oka, T., Iwata, M., Maezawa, H., et al., 2004, *ApJ*, 602, 803
- Sakai, T., Oka, T., & Yamamoto, S., 2005, in preparation.
- Sekimoto, Y., Yoshida, H., Hirota, T., et al., 1996, *Int. J. IR & MM Waves*, 17, 1263
- Sekimoto, Y., Tatematsu, K., et al., 1999, Star Formation 1999, Proceedings of Star Formation 1999, held in Nagoya, Japan, June 21 - 25, 1999, Editor: T. Nakamoto, Nobeyama Radio Observatory, 86-87
- Sekimoto, Y., et al., 2000, *Rev. Sci. Instrum.*, 71, 2895
- Shi, S. C., Noguchi, T., & Inatani, J., 1997, *IEEE Trans. on Applied Superconductivity*, 7, 2587
- Shi, S. C., Noguchi, T., Inatani, J., & Sato, T., 1998, *Internat. Symp. on Space Terehertz Technology*, Pasadena, CA
- Suzuki, H., Yamamoto, S., Ohishi, M., et al., 1992, *ApJ*, 392, 551
- Tielens, A. G. G. M., & Hollenbach, D., 1985, *ApJ*, 291, 722
- Yamamoto, S., Maezawa, H., Ikeda, M. et al., 2001, *ApJ*, 547, L165